Fatty acid-induced lipid accumulation promotes radiosensitization in Huh7 hepatocellular carcinoma cells

HARUTO TANAKA[1], YASUSHI MARIYA[2] and SATORU MONZEN[1,3]

[1]Department of Radiation Science, Hirosaki University Graduate School of Health Sciences, Hirosaki, Aomori 036-8564, Japan;
[2]Center for Cancer Treatment and Examination, Aomori Rosai Hospital, Hachinohe, Aomori 031-8551, Japan;
[3]Research Center for Biomedical Sciences, Hirosaki University, Hirosaki, Aomori 036-8564, Japan

Received September 18, 2025; Accepted December 31, 2025

DOI: 10.3892/ol.2026.15487

Abstract. Hepatocellular carcinoma (HCC), a leading cause of cancer-related mortality, represents a substantial global health burden, and the therapeutic efficacy of radiotherapy remains highly variable among patients with the condition. Metabolic alterations, particularly in lipid metabolism, may modulate radiosensitivity, although the underlying mechanisms are not fully understood. The present study investigated the impact of fatty acid uptake on radiosensitivity in HCC using the Huh7 cell line. Oleic acid (OA), a monounsaturated fatty acid, was used to induce intracellular lipid accumulation. Flow cytometry analyses revealed that OA treatment (1 mM; 18 h) considerably increased lipid content without inducing cytotoxicity. When combined with X-ray irradiation (10 Gy), OA pretreatment considerably enhanced cell death, as indicated by an increased proportion of propidium iodide-positive cells. This effect was associated with elevated levels of lipid hydroperoxides and reactive oxygen species, suggesting oxidative stress-mediated mechanisms. Furthermore, mRNA expression analyses revealed marked upregulation of ChaC glutathione specific γ-glutamylcyclotransferase 1, a gene involved in glutathione degradation and ferroptosis, in OA-treated cells. The expression levels of glutathione peroxidase 4 and glutamate-cysteine ligase catalytic subunit, key antioxidant defense genes, were also upregulated by OA and irradiation. These findings indicate that OA-induced lipid accumulation sensitized HCC cells to radiation through enhanced oxidative stress and lipid peroxidation. However, as the present study was based on an *in vitro* model using a single cell line, the potential clinical relevance of these findings remains speculative and requires further validation in *in vivo* models and clinical studies.

Correspondence to: Professor Satoru Monzen, Department of Radiation Science, Hirosaki University Graduate School of Health Sciences, 66-1 Hon-cho, Hirosaki, Aomori 036-8564, Japan
E-mail: monzens@hirosaki-u.ac.jp

Key words: hepatocellular carcinoma, oleic acid, lipid accumulation, oxidative stress, ferroptosis, radiosensitization

Introduction

Hepatocellular carcinoma (HCC) accounts for approximately 80% of primary liver malignancies, and it is the third-leading cause of cancer-related deaths worldwide (1). Although surgical resection, radiofrequency ablation, systemic therapy, and radiotherapy are available treatment options, patients with advanced-stage HCC face limited therapeutic choices and poor prognoses (2). Recent advancements in high-precision radiation techniques, such as stereotactic body radiation therapy (SBRT), have demonstrated improved local control and survival rates in patients with HCC (3). Consequently, the latest 2025 edition of the Japanese guidelines for HCC now includes radiotherapy as an optional treatment modality, highlighting its growing importance in HCC management (4). However, radiotherapy outcomes vary remarkably among individuals. Notably, the risk factors for HCC have shifted from viral hepatitis (HBV/HCV) to nonviral metabolic diseases, particularly those associated with lipid metabolism abnormalities (5,6). According to multiple studies, HCC etiology influences the treatment response, including the efficacy of radiotherapy; however, the underlying mechanisms remain unclear (7,8). Therefore, elucidating how lipid metabolism affects radiosensitivity in HCC cells is of clinical relevance.

Lipids are essential components of cell membranes and energy metabolism (9). However, excessive lipid accumulation may induce oxidative stress and lipid peroxidation, leading to various forms of cell death (10). Oleic acid (OA), a dietary monounsaturated fatty acid, induces lipid accumulation and oxidative damage in cells (11-13). Nonetheless, its impact on cancer cell radiosensitivity remains poorly understood.

During radiotherapy, nutritional management is essential to maintain treatment continuity and avoid worsening of the patient's condition. Clinical guidelines recommend personalized dietary counseling and the use of oral nutritional supplements to ensure adequate dietary intake (14). Notably, recent studies have reported that ketogenic diets, which are rich in lipids and poor in carbohydrates, can enhance oxidative stress and improve the therapeutic response to radiotherapy in animal models of lung and pancreatic cancer (15,16). These findings underscore the potential role of lipid metabolic status in radiosensitivity modulation.

This study aimed to evaluate, *in vitro*, the effects of dietary lipid uptake on the therapeutic efficacy of radiotherapy in HCC, using OA to model lipid accumulation. Our ultimate goal is to optimize radiotherapy by incorporating considerations of dietary management and lipid metabolism.

Materials and methods

In vitro cell culture. The human HCC cell line Huh7 was obtained from the RIKEN BioResource Research Center. Cells were cultured in low-glucose Dulbecco's modified Eagle medium (DMEM; FUJIFILM Wako Pure Chemical Corporation) supplemented with 10% heat-inactivated fetal bovine serum (FBS; Japan Bioserum) and 1% penicillin-streptomycin (Thermo Fisher Scientific, Inc.). Cultures were maintained at 37˚C in a humidified incubator with 5% CO_2 and 95% air. To induce lipid accumulation, Huh7 cells were cultured in low-glucose DMEM supplemented with 5% heat-inactivated FBS and 1% penicillin-streptomycin and treated with OA at concentrations ranging from 0.5 to 2 mM. OA was dissolved in 70% ethanol and added to the medium at the desired final concentrations. Control cells received an equivalent volume of 70% ethanol without OA. OA was dissolved in 70% ethanol, and an equivalent concentration of ethanol was added to all control groups. Ethanol alone did not significantly affect cell viability, lipid accumulation, or oxidative stress parameters under the experimental conditions used.

Exposure to ionizing radiation (IR). X-ray irradiation was performed using an X-ray generator (MBR-1520R-3; Hitachi Medical Co., Ltd.) operated at 150 kVp and 20 mA, with 0.5-mm aluminum and 0.3-mm copper filters. The source-to-sample distance was set at 45 cm. The delivered dose was measured using a thimble-type ionization chamber dosimeter placed adjacent to the samples during irradiation. The dose rate was 1 Gy/min. The 10 Gy dose was selected as a mechanistic *in vitro* model to reliably induce oxidative stress and lipid peroxidation, based on prior radiobiological studies and preliminary dose-response experiments, rather than to directly mimic clinical dose regimens.

Cell cycle distribution analysis. Cells were seeded in 35-mm culture dishes (2 ml of medium per dish) and subjected to X-ray irradiation at a dose of 5 Gy. Following irradiation, the cells were incubated for 3, 6, 12, 18, or 24 h. At each time point, cells were harvested and fixed with 70% ethanol precooled to -20˚C. After fixation, the cells were treated with RNase I (3.6 μg/ml; Merck KGaA) at 37˚C for 20 min in the dark. Propidium iodide (PI; 37 μg/ml) was then added, and DNA content was analyzed immediately by flow cytometry using a Cell Lab Quanta™ SC MPL system (Beckman Coulter, Inc.). The proportions of cells in the Sub-G1, G0/G1, S, and G2/M phases were calculated using Kaluza analysis software (version 2.1; Beckman Coulter, Inc.).

Measurement of lipid accumulation. Intracellular lipid accumulation was quantified using Nile red stain (FUJIFILM Wako Pure Chemical Corporation). A 1 mM stock solution of Nile red was prepared by dissolving the dye in DMSO. To assess time-dependent lipid accumulation, cells were seeded in 60-mm culture dishes (4 ml medium per dish) and treated the following day with 1 mM OA. Cells were incubated for 3, 6, 12, 18, 24, 36, or 48 h. After incubation, cells were harvested, fixed with 4% paraformaldehyde, resuspended in PBS, and stored at -20˚C. For measurement, cells were incubated with Nile red at a final concentration of 0.1 μg/ml in PBS at 37˚C for 15 min in the dark. Fluorescence intensity was measured by flow cytometry using the Cell Lab Quanta™ SC MPL system (Beckman Coulter, Inc.) and analyzed using Kaluza analysis software (version 2.1; Beckman Coulter, Inc.). To assess concentration-dependent lipid accumulation, cells were similarly seeded in 60-mm dishes and treated the following day with 0.5, 1, or 2 mM OA for 18 h. Cells were then fixed with 4% paraformaldehyde, washed with PBS, and stored at -20˚C. Staining and fluorescence measurement were performed as described above.

Measurement of the viable cell number. To evaluate the cytotoxicity of OA, cell viability was assessed using the trypan blue exclusion assay. Cells were collected from the same dishes used in the concentration-dependent lipid accumulation experiments.

Analysis of cell death. Cell death induced by OA treatment or X-ray irradiation was analyzed using direct immunofluorescence-based flow cytometry with the Cell Lab Quanta™ SC MPL system (Beckman Coulter, Inc.). Cells collected using a single pipette were washed twice with Annexin V binding buffer (cat. no. 422201; BioLegend, Inc.), after which they were stained according to the manufacturer's protocol. Fluorescein isothiocyanate (FITC)-conjugated Annexin V (cat. no. 640906; BioLegend, Inc.) and PI (MilliporeSigma) were added to the cell suspension. Fluorescence intensity was quantified by flow cytometry and analyzed using Kaluza analysis software (version 2.1; Beckman Coulter, Inc.).

Measurement of intracellular LOOH levels. Intracellular LOOH levels were measured using Liperfluo staining solution (Dojindo Laboratories, Inc.). Untreated cells or cells pretreated with OA and/or exposed to X-ray irradiation were incubated with 1 μM Liperfluo at 37˚C for 30 min in the dark. After staining, cells were collected and analyzed by flow cytometry using the Cell Lab Quanta™ SC MPL system (Beckman Coulter, Inc.). Fluorescence intensity was quantified using Kaluza analysis software (version 2.1; Beckman Coulter, Inc.).

Measurement of intracellular ROS levels. Intracellular ROS levels were measured using the fluorescent probe 2',7'-dichlorodihydrofluorescein diacetate (DCFH-DA; Dojindo Laboratories, Inc.). Cells were washed twice with Hanks' balanced salt solution (HBSS) and then incubated with a working solution of DCFH-DA at 37˚C in a humidified atmosphere of 95% air and 5% CO_2 for 30 min. After incubation, cells were washed twice with HBSS and collected. ROS levels were analyzed by flow cytometry using the Cell Lab Quanta™ SC MPL system (Beckman Coulter, Inc.). The excitation and emission wavelengths were set at 488 and 530 nm, respectively.

Analysis of mRNA expression. Total RNA was extracted from cultured cells using the RNeasy® Plus Mini Kit (Qiagen),

Table I. Sequences of human *GCLC*, *GPX4*, *CHAC1* and *ACTB* quantitative PCR primers.

Accession number	Primer name	Primer sequence (5'-3')
NM_001498.4	*GCLC* forward	CATTGATTGTCGCTGGGGAG
	GCLC reverse	CTGGGCCAGGAGATGATCAA
NM_002085.5	*GPX4* forward	AGAGATCAAAGAGTTCGCCGC
	GPX4 reverse	TCTTCATCCACTTCCACAGCG
NM_024111.6	*CHAC1* forward	TGTGGTGACGCTCCTTGAAG
	CHAC1 reverse	GCCTCTCGCACATTCAGGTAC
NM_001101.5	*ACTB* forward	GGACTTCGAGCAAGAGATGG
	ACTB reverse	AGCACTGTGTTGGCGTACAG

GCLC, glutamate-cysteine ligase catalytic subunit; *GPX4*, glutathione peroxidase 4; *CHAC1*, ChaC glutathione specific γ-glutamylcyclotransferase 1; *ACTB*, actin β.

and RNA concentrations and purity were determined using a NanoDrop spectrophotometer (Thermo Fisher Scientific, Inc.). First-strand complementary DNA (cDNA) was synthesized from total RNA using the ReverTra Ace® qPCR RT Master Mix (Toyobo Co., Ltd.) according to the manufacturer's instructions.

Quantitative PCR was performed using the Power SYBR™ Green PCR Master Mix (Applied Biosystems, Thermo Fisher Scientific) and the SmartCycler® II system (Takara Bio Inc.). Thermal cycling was performed as follows: initial denaturation at 95˚C for 10 min, followed by 40 cycles of 95˚C for 15 sec and 60˚C for 1 min. The relative expression levels of glutamate-cysteine ligase catalytic subunit (*GCLC*), glutathione peroxidase 4 (*GPX4*), and ChaC glutathione specific γ-glutamylcyclotransferase 1 (*CHAC1*) were normalized to those of β-actin (*ACTB*) and calculated using the $2^{-\Delta\Delta Cq}$ method (17).

Gene-specific primers were designed using Primer3 software and synthesized by Eurofins Genomics. Gene sequences were obtained from the NCBI Gene database (https://www.ncbi.nlm.nih.gov/gene/), and the following accession numbers were used: *GCLC* (NM_001498.4), *GPX4* (NM_002085.5), *CHAC1* (NM_024111.6), and *ACTB* (NM_001101.5) (Table I).

Statistical analysis. All statistical analyses were performed using R software (version 4.4.1; R Foundation for Statistical Computing). For comparisons among multiple groups, one-way analysis of variance (ANOVA) was used, followed by the Tukey-Kramer post hoc test. Normality and homogeneity of variance were confirmed prior to ANOVA. Analyses were applied to datasets including cell cycle distribution, lipid accumulation, cytotoxicity, LOOH levels, ROS levels, and mRNA expression. A P-value of <0.05 was considered statistically significant. All experiments were independently repeated using separate cell cultures (biological replicates). For each biological replicate, measurements were performed in duplicate or triplicate as technical replicates where applicable.

Results

Radiation-induced alteration of cell cycle distribution in Huh7 cells. To investigate the effect of IR on cell cycle progression in HCC cells, Huh7 cells were exposed to 5 Gy X-ray irradiation, and the cell cycle distribution was assessed at 3, 6, 12, 18, and 24 h post-irradiation using PI staining and flow cytometry. A marked accumulation of cells in the G2/M phase was observed at 12 h (37.7±3.5%, P<0.001) and 18 h (35.6±2.0%, P<0.001) compared with the non-irradiated controls (19.5±2.1%) (Fig. 1A). In contrast, no remarkable changes were detected at 3 h or 6 h, whereas a nonsignificant increase was noted at 24 h. Representative histograms of PI-stained cells are shown in Fig. 1B. These findings indicate that Huh7 cells undergo a robust G2/M phase arrest following DNA damage, supporting their use as a reliable *in vitro* model for studying radiotherapeutic responses. Based on these results, a post-irradiation time point of 12 h was selected for downstream analyses to capture the peak DNA damage response.

OA-induced time- and dose-dependent lipid accumulation. Huh7 cells were treated with 1 mM OA, and intracellular lipid accumulation was assessed at 3, 6, 12, 18, 24, 36, and 48 h using Nile red staining and flow cytometry. Compared to the untreated control (2.9±0.1), OA-treated cells exhibited remarkably increased lipid levels at all time points (3 h: 6.3±0.4; 6 h: 8.0±0.7; 12 h: 16.5±0.3; 18 h: 23.5±0.7; 24 h: 14.7±0.2; 36 h: 17.6±0.3; 48 h: 13.3±0.6; P<0.001 for all) (Fig. 2A and B). The highest lipid accumulation was observed at 18 h. Next, cells were exposed to OA at concentrations of 0.5, 1 or 2 mM for 18 h, and intracellular lipid levels were analyzed. Cell viability was evaluated using the trypan blue exclusion assay under the same conditions. A marked reduction in viability was detected at 2 mM OA (61.2±3.8%) compared with 0 mM (91.9±2.1%), 0.5 mM (90.0±3.6%) and 1 mM (86.1±6.2%) (P<0.001) (Fig. 2C). In addition, a dose-dependent increase in intracellular lipid-associated Nile red fluorescence intensity was observed (0 mM: 3.04; 0.5 mM: 12.7; 1 mM: 20.5; 2 mM: 29.6) (Fig. 2D and E).

Cytotoxic effect of OA in Huh7 cells. To further assess the cytotoxicity of OA, Huh7 cells were treated with 0.5, 0.75, 1, or 2 mM OA for 18 h, followed by annexin V/PI double staining and flow cytometry. A remarkable increase in the proportion of PI-positive (necrotic/late apoptotic) cells was observed only in the 2-mM group (50.0±17.1%) compared to the untreated

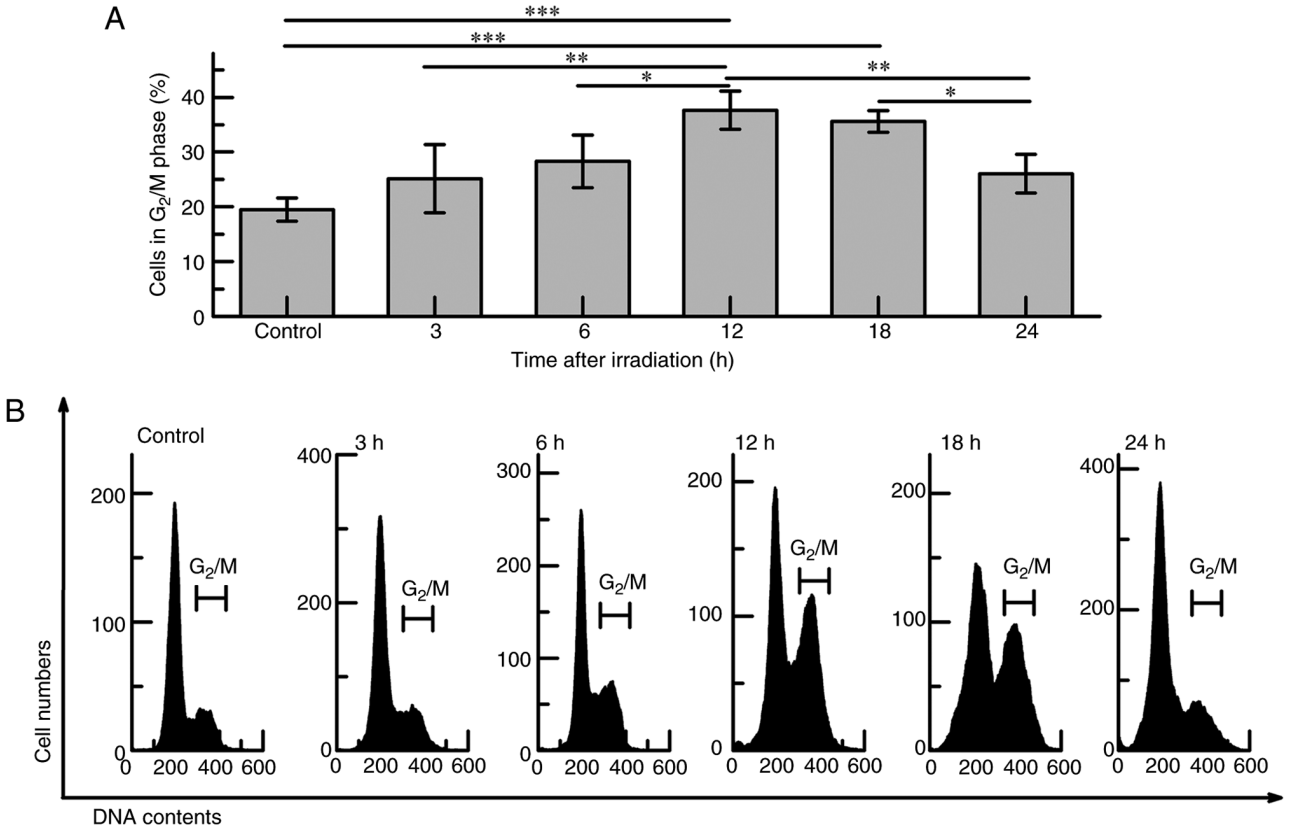

Figure 1. Radiation-induced G_2/M arrest in Huh7 cells. (A) Cell cycle distribution of Huh7 cells following 5 Gy X-ray irradiation. The proportion of cells in the G_2/M phase was determined at 3, 6, 12, 18 and 24 h post-irradiation using flow cytometry. Data are presented as the mean ± SD from four independent experiments. *P<0.05, **P<0.01 and ***P<0.001 vs. non-irradiated control. (B) Representative histograms of DNA content assessed by PI staining at each time point. Statistical analysis was performed using one-way ANOVA followed by the Tukey-Kramer post hoc test.

control group (18.2±8.0%, P<0.05). No statistically significant differences were detected in the 0.5-mM (10.8±6.0%), 0.75-mM (20.6±6.8%), or 1-mM (26.8±10.1%) groups (Fig. 3). These results confirm that 1 mM OA does not induce substantial cytotoxicity, indicating its suitability for use as a sublethal dose for subsequent mechanistic studies.

OA enhances radiation-induced cell death. To investigate whether OA-induced lipid accumulation enhances the cytotoxic effect of ionizing radiation (IR), Huh7 cells were pretreated with 1 mM OA for 18 h prior to X-ray irradiation at doses ranging from 1 to 10 Gy. Cell death was assessed 12 h post-irradiation using annexin V/PI staining and flow cytometry. At 10 Gy, the proportion of PI-positive cells was remarkably higher in the OA-pretreated group (17.9±7.8%) than in the IR-only group (10.7±0.8%, P<0.05), indicating enhanced cell membrane damage (Fig. 4A). No remarkable differences were observed at lower radiation doses. These findings suggest that OA-induced lipid accumulation sensitizes Huh7 cells to radiation-induced cell death in a dose-dependent manner, particularly at higher radiation doses. The 10-Gy dose was selected for subsequent mechanistic analyses because a significant increase in PI-positive cells was observed only at this dose when OA pretreatment was combined with irradiation, compared with irradiation alone (Fig. 4A and B). In addition, previous *in vitro* radiobiology studies have commonly employed single high-dose irradiation to robustly induce oxidative stress and lipid peroxidation, facilitating mechanistic evaluation of radiation-induced cell death pathways (18,19).

OA augments oxidative stress and lipid peroxidation after IR exposure. To elucidate the mechanism underlying OA-mediated radiosensitization, we measured the levels of intracellular oxidative stress markers, including LOOH and ROS. LOOH levels, assessed by Liperfluo staining, were not remarkably altered by OA treatment alone (473.3±14.9) compared to the untreated control. In contrast, 10 Gy X-ray irradiation remarkably increased LOOH levels (487.5±31.6, P<0.05). Notably, OA pretreatment combined with 10 Gy irradiation further elevated LOOH accumulation (541.4±2.1, P<0.05 vs. 10 Gy alone) (Fig. 5A). These findings indicate that OA treatment augments radiation-induced lipid peroxidation. Moreover, ROS levels were remarkably increased by OA alone (42.0±10.3) compared to control (24.1±8.2, P<0.05), as presented in Fig. 6.

Modulation of oxidative stress-related gene expression by OA and IR. To further elucidate the molecular mechanisms underlying OA-mediated radiosensitization, we analyzed the expression of key oxidative stress-related genes: *GCLC*, *GPX4*, and *CHAC1*. Irradiation alone remarkably upregulated *GCLC* expression (2.5±1.0-fold, P<0.05), whereas OA administration alone had no statistically significant effect. The combination of OA and irradiation did not further increase the GCLC expression beyond that induced by irradiation alone

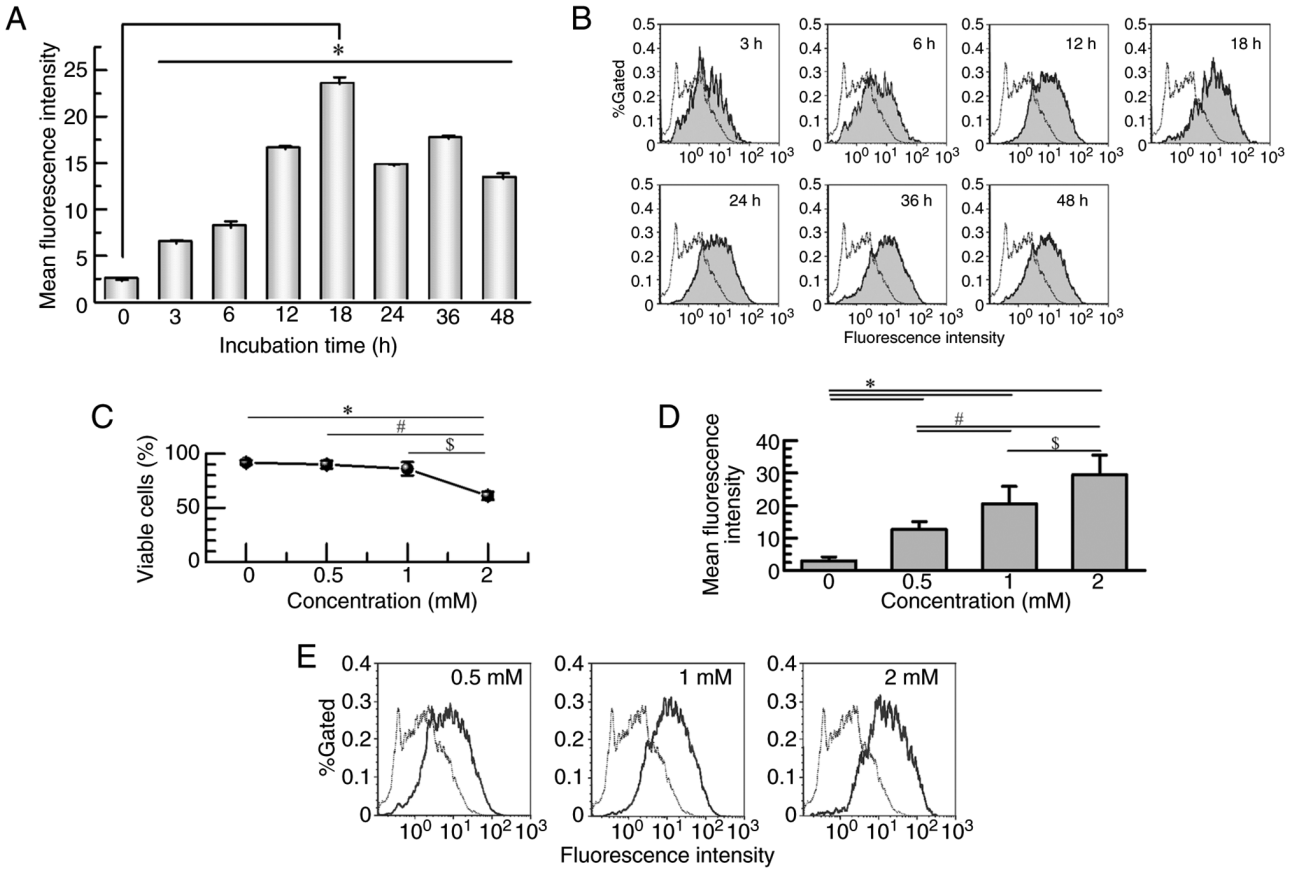

Figure 2. OA-induced time- and dose-dependent lipid accumulation in Huh7 cells. (A) Time-course analysis of intracellular lipid accumulation following treatment with 1 mM OA. Lipid content was measured at 3, 6, 12, 18, 24, 36 and 48 h using Nile red staining and flow cytometry. Data are presented as the mean ± SD from four independent experiments. *P<0.001 vs. untreated control (0 h). (B) Representative histograms of Nile red fluorescence showing a time-dependent increase in lipid accumulation. The dashed line represents the untreated control (0 h). (C) Quantification of cell viability following 18-h treatment with 0.5, 1 or 2 mM OA, determined using the trypan blue exclusion assay, in which viable and non-viable cells were manually counted under a light microscope using a Bürker-Türk hemocytometer. Continuous data are presented as the mean ± SD of three independent experiments. *P<0.001 vs. 0 mM, #P<0.001 vs. 0.5 mM and $P<0.001 vs. 1 mM. (D) Quantification of intracellular lipid content following 18-h treatment with 0.5, 1 or 2 mM OA. Data are presented as the mean ± SD of three independent experiments. *P<0.001 vs. 0 mM, #P<0.001 vs. 0.5 mM and $P<0.001 vs. 1 mM. Lipid content was assessed by Nile red staining. (E) Representative histograms of Nile red fluorescence showing dose-dependent lipid accumulation. The dashed line represents the untreated control (0 mM). Statistical analysis was performed using one-way ANOVA followed by the Tukey-Kramer post hoc test. OA, oleic acid.

(2.2±0.4-fold, P<0.05) (Fig. 7A). In contrast, *GPX4* expression was remarkably upregulated in all treatment groups-OA alone (2.4±0.1, P<0.01), IR alone (2.3±0.8, P<0.05), and the OA + IR combination (2.8±0.5, P<0.01) (Fig. 7B). Notably, the levels of *CHAC1*, a glutathione-degrading enzyme and marker of ferroptosis, were markedly induced by OA treatment alone (4.1±0.6-fold, P<0.01) and further elevated in the OA + IR group (6.8±1.4-fold, P<0.001); however, it was not affected by IR alone (Fig. 7C). These transcriptional changes suggest that OA enhances radiation-induced oxidative stress and may contribute to ferroptosis-related signaling pathways.

Discussion

In this study, we established an *in vitro* model using Huh7 HCC cells and OA, a monounsaturated fatty acid, to investigate how lipid accumulation affects radiosensitivity. OA pretreatment at 1 mM for 18 h (resulting in maximal lipid accumulation without overt cytotoxicity) followed by 10 Gy X-ray irradiation remarkably increased the proportion of PI-positive cells and intracellular LOOH compared to radiation alone. These findings indicate that OA enhances radiation-induced cell death via additive effects on oxidative membrane damage.

IR primarily targets nuclear DNA and can induce cell cycle arrest and apoptosis, particularly at the G2/M checkpoint, which is known to be the most radiosensitive phase (20,21). In our experiments, a marked accumulation of Huh7 cells in the G2/M phase was observed 12 h post-irradiation, validating this time point as optimal for subsequent analyses.

OA and other long-chain fatty acids, such as palmitic acid, have been widely used in *in vitro* lipid metabolism studies. Previous studies have demonstrated that fatty acid treatment at 0.5-2 mM concentrations for 12-24 h induces lipid accumulation without affecting viability up to 1 mM (22-24). Consistent with this, we demonstrated that administration of 1 mM OA for 18 h maximized lipid accumulation in Huh7 cells without inducing cytotoxicity, as confirmed by Nile red staining and annexin V/PI analyses.

Notably, while the number of annexin V-positive cells (a marker of early apoptosis) was not remarkably increased, those of PI-positive cells were elevated upon OA + IR co-treatment, suggesting enhanced necrotic or non-apoptotic cell death. OA

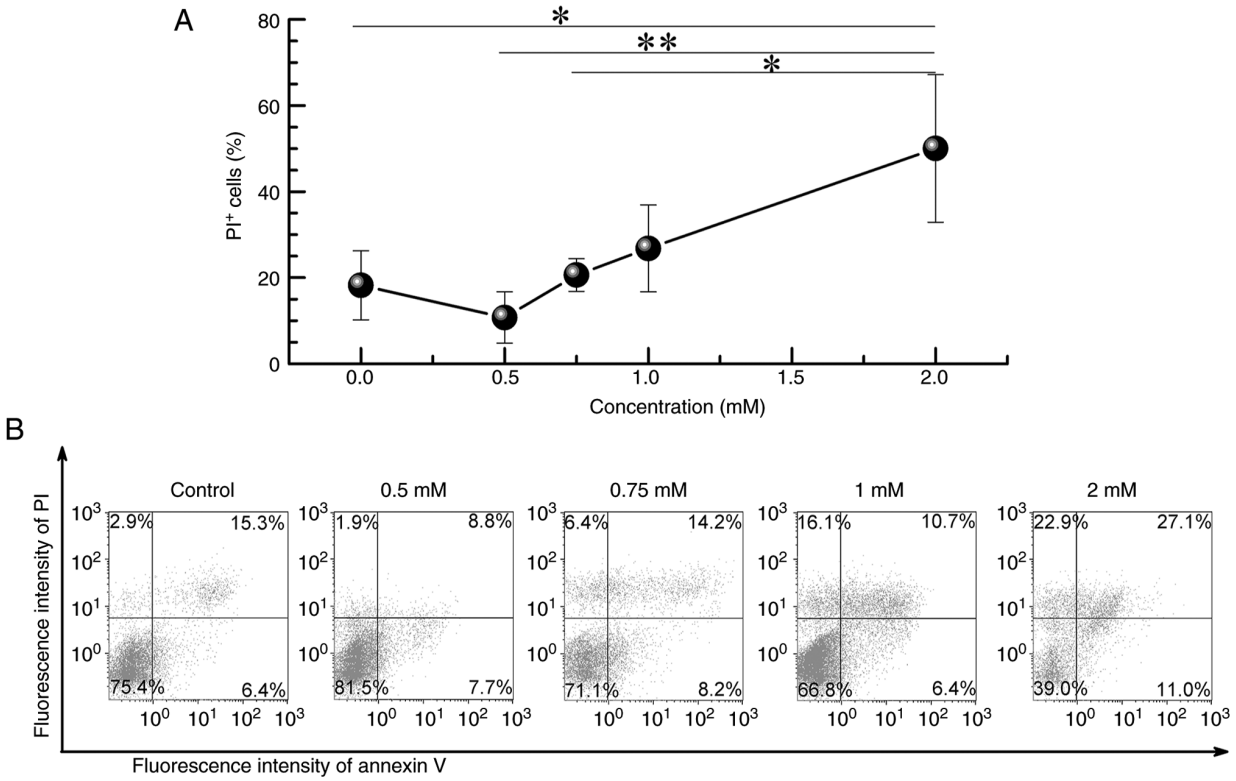

Figure 3. Cytotoxic effect of OA in Huh7 cells. (A) Quantification of PI-positive cells following 18-h treatment with 0.5, 0.75, 1 or 2 mM OA using annexin V/PI staining and flow cytometry. Continuous data are presented as the mean ± SD from three independent experiments. *P<0.05 and **P<0.01 as indicated. (B) Representative flow cytometry plots illustrating annexin V and PI staining profiles across different OA concentrations. Statistical analysis was performed using one-way ANOVA followed by the Tukey-Kramer post hoc test. OA, oleic acid.

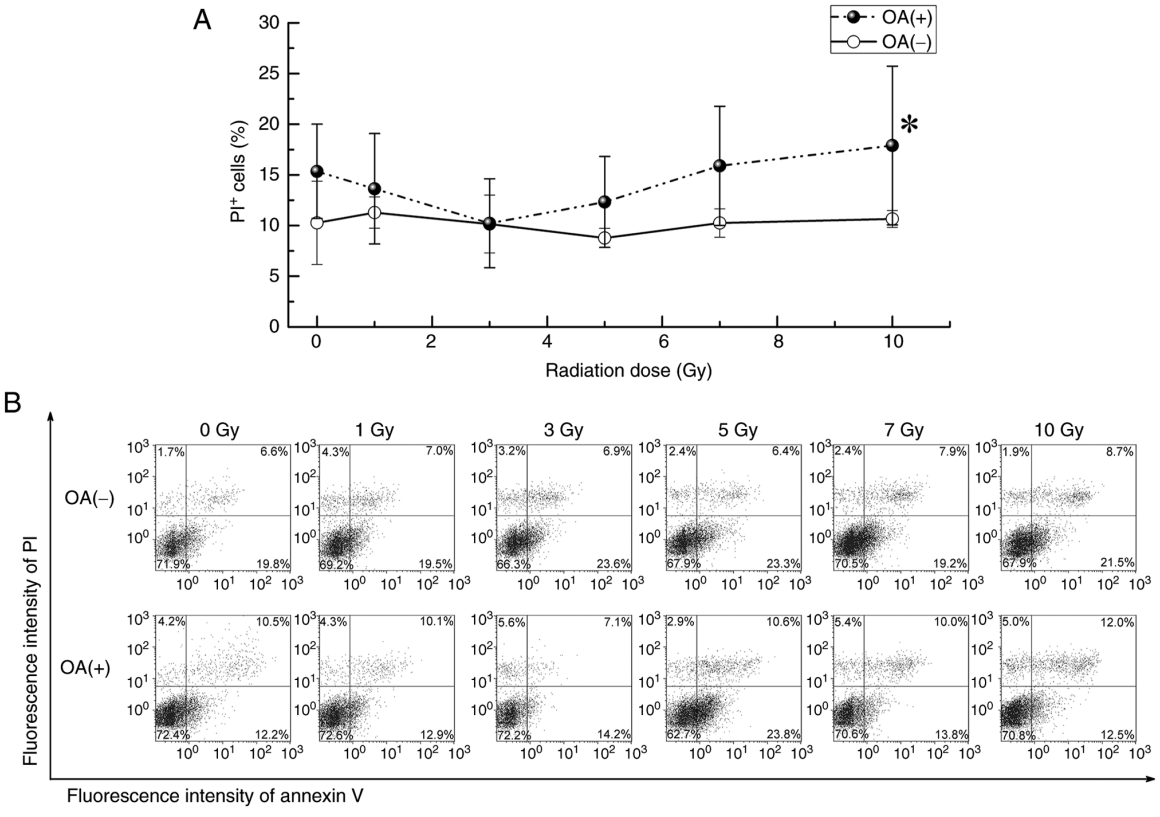

Figure 4. OA enhances radiation-induced cell death in Huh7 cells. (A) Quantification of PI-positive cells following 1-10 Gy X-ray irradiation with or without OA pretreatment (1 mM for 18 h). Cell death was assessed by annexin V/PI staining 12 h post-irradiation. Continuous data are presented as the mean ± SD from eight independent experiments. *P<0.05 vs. 10 Gy without OA. (B) Representative flow cytometry plots of annexin V and PI staining in irradiated cells with or without OA pretreatment. Statistical analysis was performed using one-way ANOVA followed by the Tukey-Kramer post hoc test. OA, oleic acid.

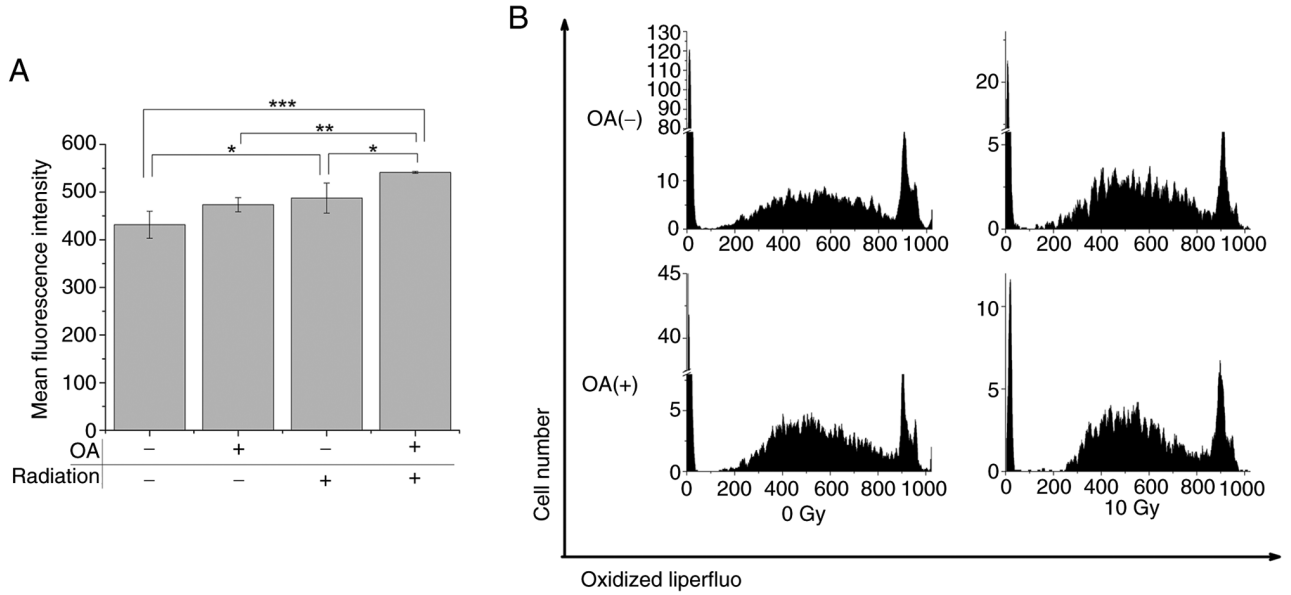

Figure 5. OA enhances radiation-induced lipid peroxidation in Huh7 cells. (A) Quantification of intracellular LOOH using Liperfluo staining following treatment with OA (1 mM; 18 h), 10 Gy X-ray irradiation or both. LOOH levels were measured 12 h post-irradiation by flow cytometry. Continuous data are presented as the mean ± SD from six independent experiments. *P<0.05, **P<0.01 and ***P<0.001 as indicated. (B) Representative histograms of Liperfluo fluorescence intensity depicting the LOOH distribution across treatment groups. Statistical analysis was performed using one-way ANOVA followed by the Tukey-Kramer post hoc test. LOOH, lipid hydroperoxides; OA, oleic acid.

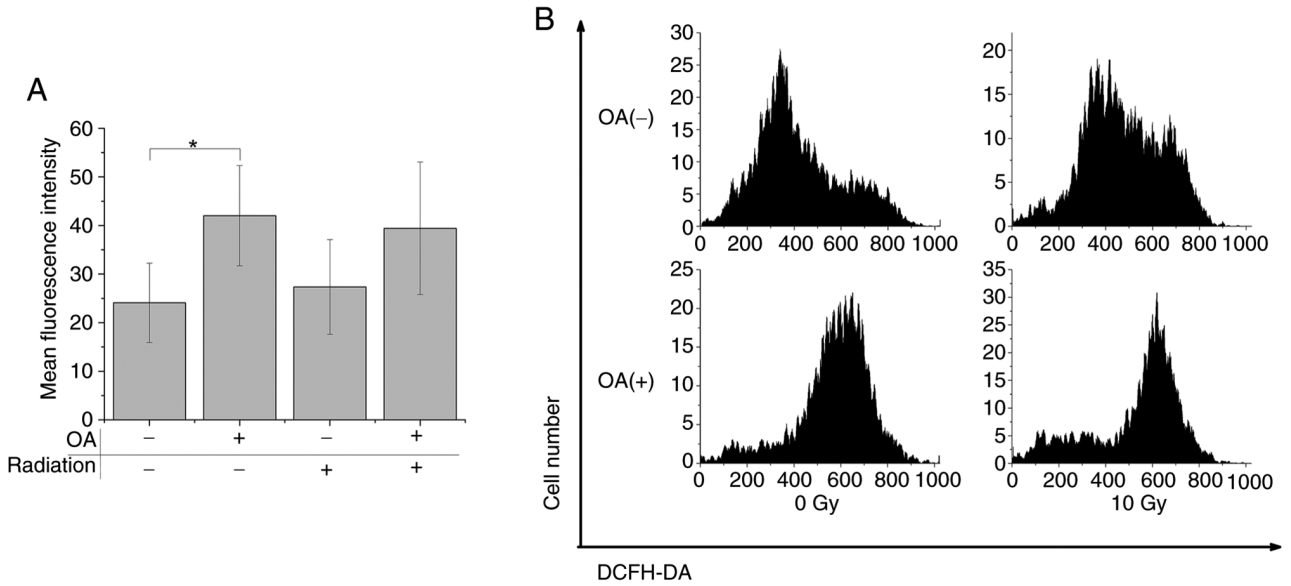

Figure 6. OA increases intracellular ROS levels in Huh7 cells. (A) Quantification of ROS levels following treatment with OA (1 mM; 18 h), 10 Gy X-ray irradiation or both. ROS levels were measured using the DCFH-DA fluorescent probe and analyzed by flow cytometry 12 h post-irradiation. Continuous data are presented as the mean ± SD of six independent experiments. *P<0.05 vs. untreated control. (B) Representative histograms of DCFH-DA fluorescence intensity showing the ROS distribution across treatment groups. Statistical analysis was performed using one-way ANOVA followed by the Tukey-Kramer post hoc test. OA, oleic acid; ROS, reactive oxygen species; DCFH-DA, 2',7'-dichlorodihydrofluorescein diacetate.

treatment alone also remarkably increased intracellular ROS levels, consistent with prior findings that OA promotes oxidative stress in hepatic cells (25). These results collectively imply that OA may sensitize HCC cells to IR-induced necrotic cell death via oxidative membrane damage and lipid peroxidation. Ionizing radiation is also known to activate inflammation-associated signaling pathways, including NF-κB-dependent and cytokine-mediated responses, which can indirectly amplify intracellular oxidative stress through enhanced ROS generation. Although inflammatory mediators were not directly assessed in the present study, the observed increase in ROS and lipid peroxidation following OA pretreatment and irradiation is consistent with inflammation-associated redox dysregulation reported in previous radiobiological studies (18,21). These considerations suggest that inflammatory signaling may indirectly contribute to oxidative stress amplification under lipid-rich conditions.

In this context, the potential involvement of lipid oxidation-related receptors, such as lectin-like oxidized low-density

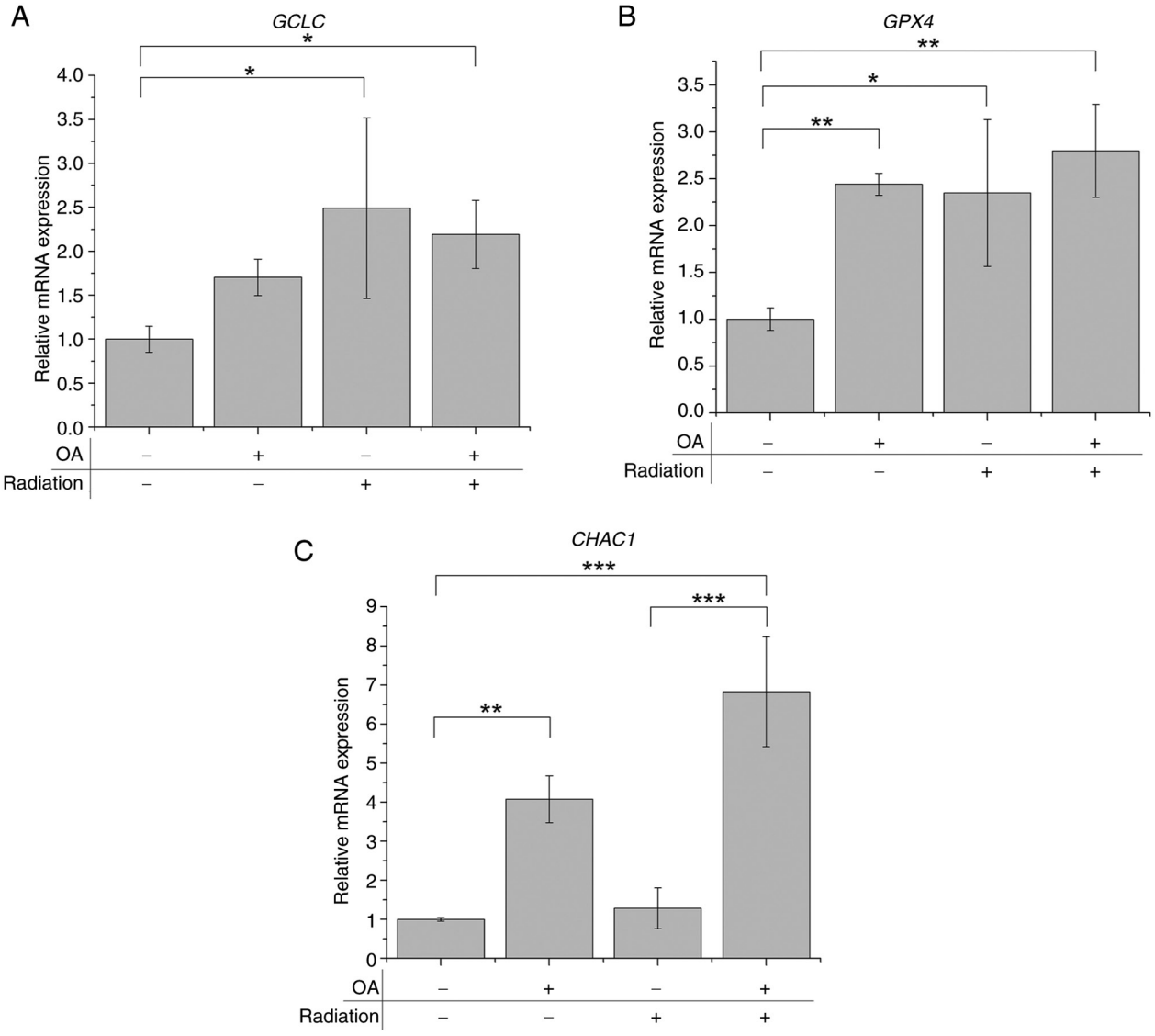

Figure 7. Modulation of oxidative stress-related gene expression by OA and irradiation in Huh7 cells. Relative mRNA expression levels of (A) *GCLC*, (B) *GPX4* and (C) *CHAC1* in Huh7 cells treated with OA (1 mM; 18 h), X-ray irradiation (10 Gy) or their combination. Gene expression was quantified by reverse transcription-quantitative PCR and normalized to *ACTB* using the $2^{-\Delta\Delta Cq}$ method. Continuous data are presented as the mean ± SD of three independent experiments. Statistical analysis was performed using one-way ANOVA followed by the Tukey-Kramer post hoc test. *P<0.05, **P<0.01 and ***P<0.001 as indicated. *CHAC1*, ChaC glutathione specific γ-glutamylcyclotransferase 1; *GCLC*, glutamate-cysteine ligase catalytic subunit; *GPX4*, glutathione peroxidase 4; OA, oleic acid.

lipoprotein receptor-1 (LOX-1), warrants consideration. LOX-1 has been reported to mediate inflammatory and oxidative responses to oxidized lipids, particularly in immune and vascular cells, and its deficiency attenuates inflammation-associated tissue damage in experimental models (26). However, in the present *in vitro* system using Huh7 cells, lipid peroxidation is most likely driven by radiation-induced non-enzymatic oxidative reactions rather than receptor-mediated uptake of oxidized lipoproteins. As LOX-1 expression or ox-LDL signaling was not examined in this study, its involvement remains speculative. Future studies may clarify whether LOX-1-related pathways contribute to radiation-induced oxidative stress under lipid-rich conditions in HCC.

To further elucidate the underlying mechanism, we evaluated the expression of oxidative stress-related genes. *GCLC* expression was upregulated by IR but not by OA, whereas that of *GPX4* was upregulated by both OA and IR. Importantly, the expression of *CHAC1* (a gene associated with glutathione degradation and ferroptosis) was remarkably induced by OA alone and further elevated by the combination of OA + IR; however, it was not induced by IR alone (27,28). These results suggest that OA may disrupt redox homeostasis by promoting glutathione consumption and degradation, thereby impairing the cellular antioxidant defense.

GPX4 requires reduced glutathione (GSH) as a cofactor to detoxify lipid peroxides such as LOOH. The depletion of GSH via *CHAC1*-mediated degradation or ROS-driven consumption can lead to ferroptotic-like cell death (18). Thus, the observed upregulation of *CHAC1* expression and the increase in LOOH in OA + IR-treated cells indicate that ferroptosis-related signaling may contribute to the enhanced radiosensitivity (19). Consistently, Ye *et al* (29) demonstrated that radiation-induced lipid peroxidation triggers ferroptosis and synergizes with ferroptosis inducers, further supporting the concept that

ferroptotic signaling underlies radiation-enhanced oxidative damage.

A major limitation of this study is the lack of functional validation via knockdown or overexpression of key regulators such as *CHAC1* and *GPX4*. Furthermore, intracellular GSH levels and *GPX4* enzymatic activity were not directly measured. In addition, the present findings are derived from a single HCC cell line (Huh7) and an *in vitro* experimental system. The absence of *in vivo* models or patient-derived samples limits the generalizability of these results. Future studies employing multiple HCC cell lines, animal models, and clinically relevant systems will be necessary to validate the broader relevance of lipid-induced radiosensitization and its potential translational implications.

Despite these limitations, the present study provides novel evidence that OA-induced lipid accumulation enhances HCC cell radiosensitivity by amplifying oxidative stress and lipid peroxidation. Importantly, OA-induced lipid accumulation alone is unlikely to be sufficient to determine radiosensitivity, and its effects become evident primarily in the context of ionizing radiation-induced oxidative stress. Thus, modulation of lipid metabolism should be regarded as a potential adjunctive factor rather than an independent therapeutic strategy. In addition, validation using multiple hepatocellular carcinoma cell lines with distinct metabolic characteristics will be required to determine the generalizability of the present findings. Further validation using *in vivo* models and clinical studies will be required before any translational or clinical implications can be considered.

Acknowledgements

Not applicable.

Funding

The present study was supported by JSPS KAKENHI, Grants-in-Aid for Scientific Research (B) (grant no. 21H02861/23K21419), Grant-in-Aid for Challenging Research (grant no. 25K22722) and Takeda Science Foundation 2023.

Availability of data and materials

The data generated in the present study are included in the figures and/or tables of this article.

Authors' contributions

HT, YM and SM designed the study, prepared the manuscript draft, and substantively participated in the manuscript revision. HT and SM analyzed all biological data. YM and SM supervised the study, critically reviewed the manuscript, and provided final approval for the version to be submitted and published. HT, YM and SM confirm the authenticity of all the raw data. All authors have read and approved the final version of the manuscript.

Ethics approval and consent to participate

Not applicable.

Patient consent for publication

Not applicable.

Competing interests

The authors declare that they have no competing interests.

References

1. Bray F, Laversanne M, Sung H, Ferlay J, Siegel RL, Soerjomataram I and Jemal A: Global cancer statistics 2022: GLOBOCAN estimates of incidence and mortality worldwide for 36 cancers in 185 countries. CA Cancer J Clin 74: 229-263, 2024.
2. Reig M, Forner A, Rimola J, Ferrer-Fàbrega J, Burrel M, Garcia-Criado Á, Kelley RK, Galle PR, Mazzaferro V, Salem R, *et al*: BCLC strategy for prognosis prediction and treatment recommendation: The 2022 update. J Hepatol 76: 681-693, 2022.
3. Kimura T, Fujiwara T, Kameoka T, Adachi Y and Kariya S: The current role of stereotactic body radiation therapy (SBRT) in hepatocellular carcinoma (HCC). Cancers (Basel) 14: 4383, 2022;
4. The Japan Society of Hepatology (ed): Clinical Practice Guidelines for Hepatocellular Carcinoma 2025. 6th Edition, Kanehara & Co., Ltd., Tokyo, Japan, pp 90, 2025 (In Japanese).
5. Younossi ZM, Golabi P, Paik JM, Henry A, Van Dongen C and Henry L: The global epidemiology of nonalcoholic fatty liver disease (NAFLD) and nonalcoholic steatohepatitis (NASH): A systematic review. Hepatology 77: 1335-1347, 2023.
6. Toh MR, Wong EYT, Wong SH, Ng AWT, Loo LH, Chow PK and Ngeow J: Global epidemiology and genetics of hepatocellular carcinoma. Gastroenterology 164: 766-782, 2023.
7. Pfister D, Núñez NG, Pinyol R, Govaere O, Pinter M, Szydlowska M, Gupta R, Qiu M, Deczkowska A, Weiner A, *et al*: NASH limits anti-tumour surveillance in immunotherapy-treated HCC. Nature 592: 450-456, 2021.
8. Shimose S, Hiraoka A, Casadei-Gardini A, Tsutsumi T, Nakano D, Iwamoto H, Tada F, Rimini M, Tanaka M, Torimura T, *et al*: The beneficial impact of metabolic dysfunction-associated fatty liver disease on lenvatinib treatment in patients with non-viral hepatocellular carcinoma. Hepatol Res 53: 104-115, 2023.
9. Bian X, Liu R, Meng Y, Xing D, Xu D and Lu Z: Lipid metabolism and cancer. J Exp Med 218: e20201606, 2021.
10. Martin-Perez M, Urdiroz-Urricelqui U, Bigas C and Benitah SA: The role of lipids in cancer progression and metastasis. Cell Metab 34: 1675-1699, 2022.
11. Li J, Wang T, Liu P, Yang F, Wang X, Zheng W and Sun W: Hesperetin ameliorates hepatic oxidative stress and inflammation via the PI3K/AKT-Nrf2-ARE pathway in oleic acid-induced HepG2 cells and a rat model of high-fat diet-induced NAFLD. Food Funct 12: 3898-3918, 2021.
12. Yang Y, Chen J, Gao Q, Shan X, Wang J and Lv Z: Study on the attenuated effect of Ginkgolide B on ferroptosis in high fat diet induced nonalcoholic fatty liver disease. Toxicology 445: 152599, 2020.
13. Zhang J, Zhang SD, Wang P, Guo N, Wang W, Yao LP, Yang Q, Efferth T, Jiao J and Fu YJ: Pinolenic acid ameliorates oleic acid-induced lipogenesis and oxidative stress via AMPK/SIRT1 signaling pathway in HepG2 cells. Eur J Pharmacol 861: 172618, 2019.
14. Muscaritoli M, Arends J, Bachmann P, Baracos V, Barthelemy N, Bertz H, Bozzetti F, Hütterer E, Isenring E, Kaasa S, *et al*: ESPEN practical guideline: Clinical nutrition in cancer. Clin Nutr 40: 2898-2913, 2021.
15. Allen BG, Bhatia SK, Buatti JM, Brandt KE, Lindholm KE, Button AM, Szweda LI, Smith BJ, Spitz DR and Fath MA: Ketogenic diets enhance oxidative stress and radio-chemo-therapy responses in lung cancer xenografts. Clin Cancer Res 19: 3905-3913, 2013.
16. Zahra A, Fath MA, Opat E, Mapuskar KA, Bhatia SK, Ma DC, Rodman SN III, Snyders TP, Chenard CA, Eichenberger-Gilmore JM, *et al*: Consuming a ketogenic diet while receiving radiation and chemotherapy for locally advanced lung cancer and pancreatic cancer: The University of Iowa experience of two phase 1 clinical trials. Radiat Res 187: 743-754, 2017.
17. Livak KJ and Schmittgen TD: Analysis of relative gene expression data using real-time quantitative PCR and the 2(-Delta Delta C(T)) method. Methods 25: 402-408, 2001.

18. Chen Z, Tian R, She Z, Cai J and Li H: Role of oxidative stress in the pathogenesis of nonalcoholic fatty liver disease. Free Radic Biol Med 152: 116-141, 2020.
19. Ursini F and Maiorino M: Lipid peroxidation and ferroptosis: The role of GSH and GPx4. Free Radic Biol Med 152: 175-185, 2020.
20. Verheij M: Clinical biomarkers and imaging for radiotherapy-induced cell death. Cancer Metastasis Rev 27: 471-480, 2008.
21. Matt S and Hofmann TG: The DNA damage-induced cell death response: A roadmap to kill cancer cells. Cell Mol Life Sci 73: 2829-2850, 2016.
22. Listenberger LL, Han X, Lewis SE, Cases S, Farese RV Jr, Ory DS and Schaffer JE: Triglyceride accumulation protects against fatty acid-induced lipotoxicity. Proc Natl Acad Sci USA 100: 3077-3082, 2023.
23. Ricchi M, Odoardi MR, Carulli L, Anzivino C, Ballestri S, Pinetti A, Fantoni LI, Marra F, Bertolotti M, Banni S, *et al*: Differential effect of oleic and palmitic acid on lipid accumulation and apoptosis in cultured hepatocytes. J Gastroenterol Hepatol 24: 830-840, 2009.
24. Wang Y, Chen C, Chen J, Sang T, Peng H, Lin X, Zhao Q, Chen S, Eling T and Wang X: Overexpression of NAG-1/GDF15 prevents hepatic steatosis through inhibiting oxidative stress-mediated dsDNA release and AIM2 inflammasome activation. Redox Biol 52: 102322, 2022.
25. Sgonc R and Gruber J: Apoptosis detection: An overview. Exp Gerontol 33: 525-533, 1998.
26. Hashimoto K, Oda Y, Nakagawa K, Ikeda T, Ohtani K and Akagi M: LOX-1 deficient mice show resistance to zymosan-induced arthritis. Eur J Histochem 62: 2847, 2018.
27. Balachander GJ, Subramanian S and Ilango K: Rosmarinic acid attenuates hepatic steatosis by modulating ER stress and autophagy in oleic acid-induced HepG2 cells. RSC Adv 8: 26656-26663, 2018.
28. Li JY, Ren C, Wang LX, Yao RQ, Dong N, Wu Y, Tian YP and Yao YM: Sestrin2 protects dendrite cells against ferroptosis induced by sepsis. Cell Death Dis 12: 834, 2021.
29. Ye LF, Chaudhary KR, Zandkarimi F, Harken AD, Kinslow CJ, Upadhyayula PS, Dovas A, Higgins DM, Tan H, Zhang Y, *et al*: Radiation-induced lipid peroxidation triggers ferroptosis and synergizes with ferroptosis inducers. ACS Chem Biol 15: 469-484, 2020.